MechSE

ANNUAL REPORT 2009

UIUC, August 5, 2009

Thermal-mechanical Behavior of the Solidifying Shell, Ideal Taper, and Longitudinal Crack Formation in a Funnel Mold

Lance C. Hibbeler
(MSME/Ph.D. Student)

Department of Mechanical Science and Engineering
University of Illinois at Urbana-Champaign

Continuous Slab Casting Molds

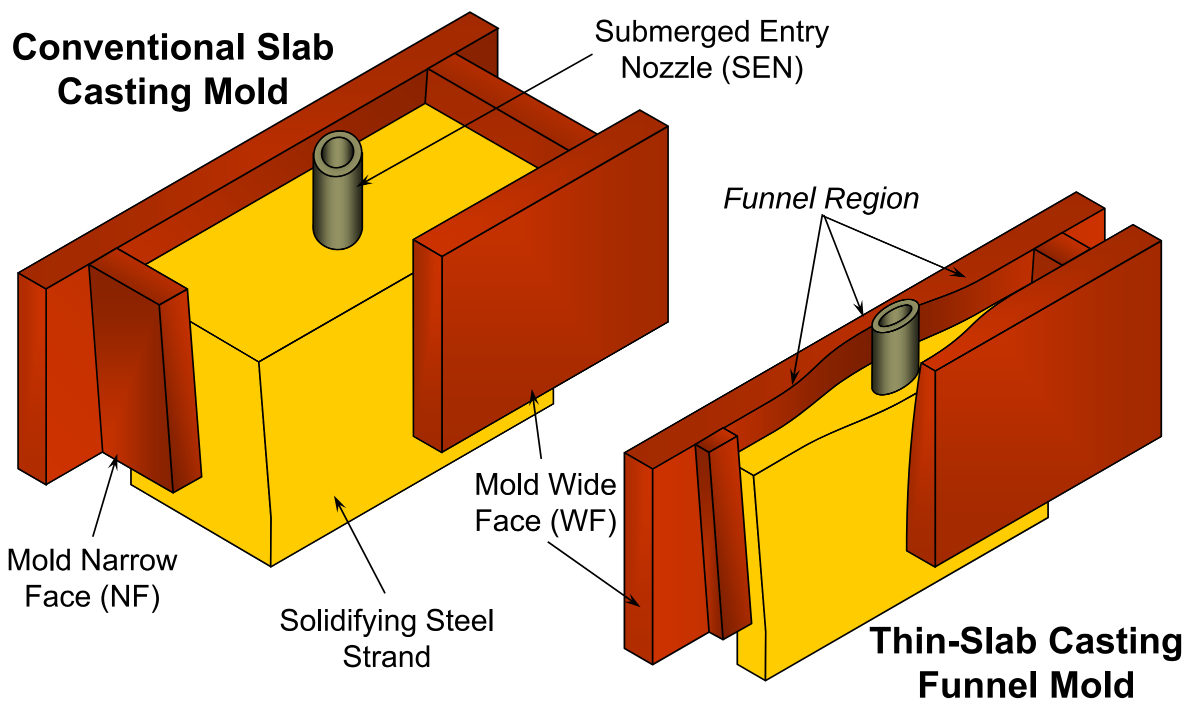

Funnel Mold Terminology and Nominal Dimensions

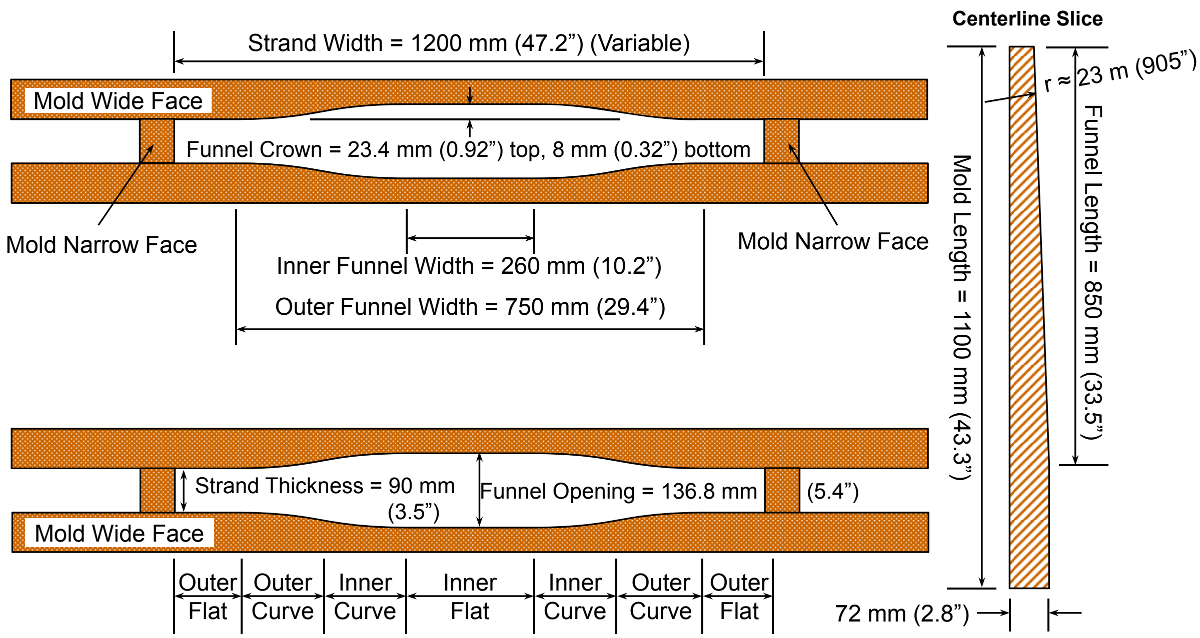

Longitudinal Facial Cracking

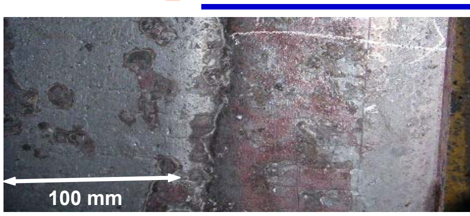

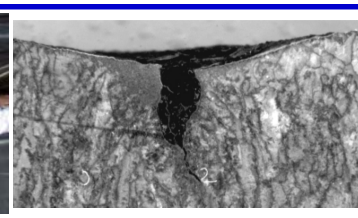

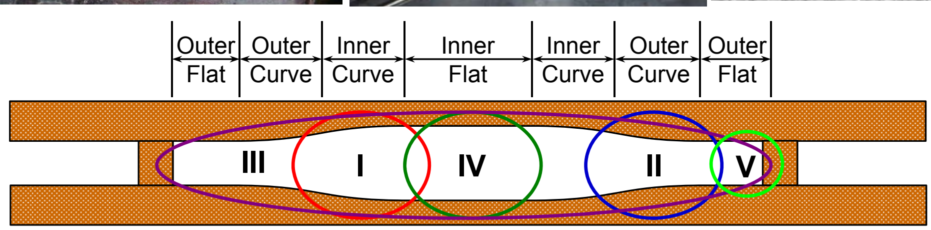

Plant Experience I

- Inside curve region
- Long cracks in root of depression
- Caused about 60% of breakouts

Plant Experience II

- Outside curve region
- Long cracks in root of depression

Plant Experience III

- Short, jagged cracks form all around perimeter
- Heat transfer related

Plant Experience IV

- Occur around SEN- fluid flow problems

Plant Experience V

- Off-corner on wide face- insufficient taper

Plant Experience I: LFC Breakout Locations

Data provided by A. Kamperman of Corus

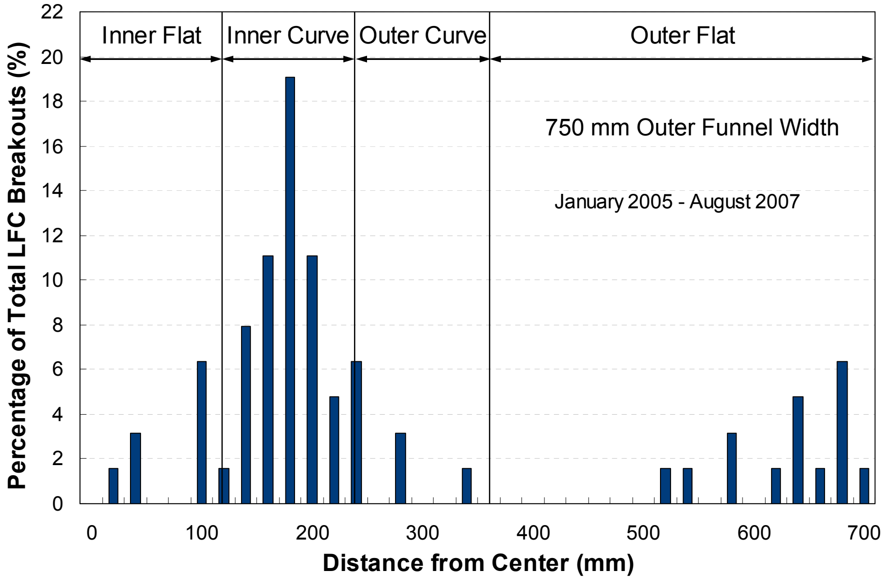

Each interval is 10 mm. Shows the locations of depression-type LFC's that caused breakouts

Longitudinal Facial Cracking: Depression Mechanism (Type I,II)

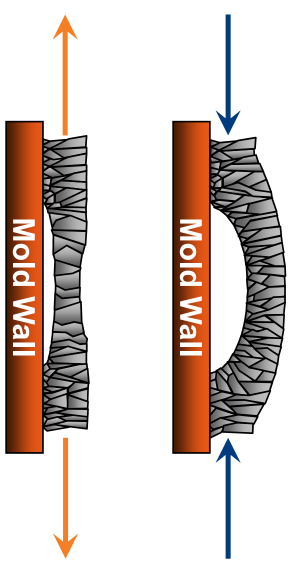

- Root cause is **non-uniform heat transfer**
- Initiate nonuniformity (shell depression)
  - Variations in slag rim thickness at meniscus
  - Gap from necking (self-correcting)
  - Gap from buckling (self-amplifying)
- Depression causes:
  - Lower heat flux
  - Higher shell temperature
    (Amplifies if buckling)
  - Thinner shell
  - Grain growth (larger grains)
  - More brittle behavior
  - Stress and strain concentrations
    (Combination causes cracks)
- Tensile inelastic strain exceeds critical value → cracks form

Numerical Model

- Coupled thermal-stress analysis with ABAQUS
  - Transient solidification heat transfer in a moving 2D slice
  - Special two-level integration scheme for elastic-viscoplastic mechanical behavior (implemented with a UMAT user subroutine)
- Thermal analysis:
  - Standard Fourier heat conduction with solidification $\rho \frac{\partial H}{\partial t} = \nabla \cdot (\boldsymbol{k} \cdot \nabla T)$
  - Temperature-dependent thermal conductivity and specific heat
- Mechanical analysis:
  - Standard mechanical (static) equilibrium, small strains $\nabla \cdot \boldsymbol{\sigma} + \boldsymbol{b} = 0$
  - Temperature- and phase- (L, δ, γ) dependent constitutive behavior
  - Temperature-dependent elastic modulus and thermal expansion
  - "Softened" exponential pressure-overclosure contact relationship
  - Interfacial friction factor of μ = 0.16 [Meng *et al.*, CMQ 45-1 pg. 79-94]
  - Ferrostatic pressure
- 2D model includes the funnel shape and mold oscillations

0.045 %C Steel Phases

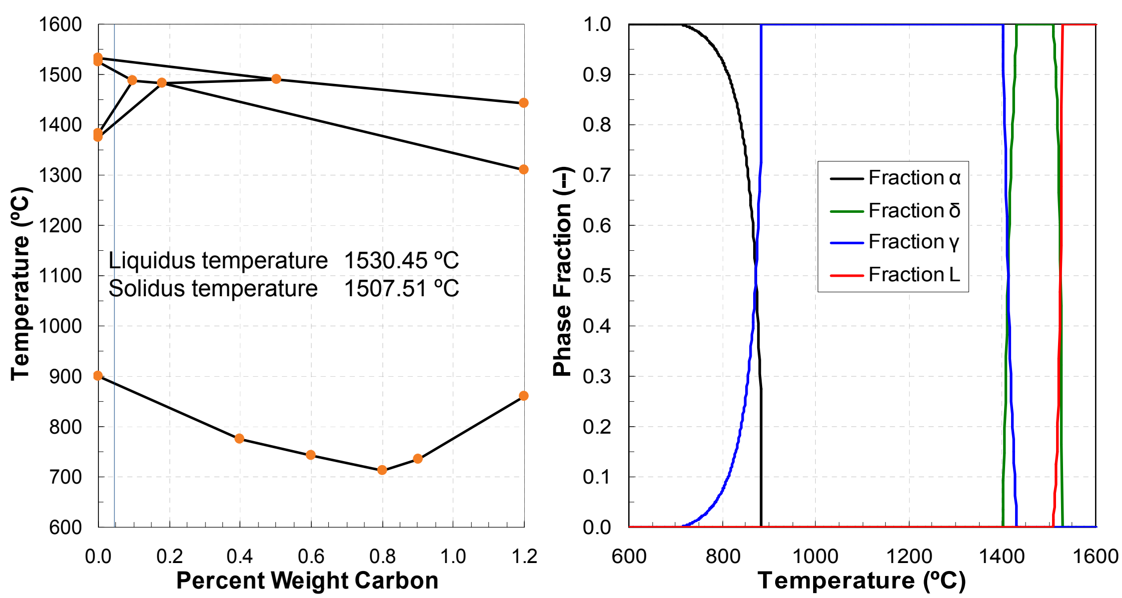

[Won and Thomas, MTB, 2001]

Constitutive Equations

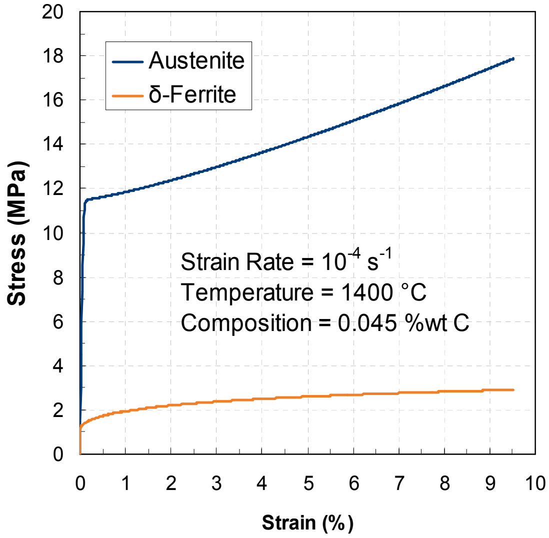

- P.F. Kozlowski, B.G. Thomas, J.A. Azzi, and H. Wang, "Simple Constitutive Equations for Steel at High Temperature." *Metallurgical and Materials Transactions*, **23A** (1992), No. 3, pg. 903-918.
- H. Zhu, "Coupled Thermo-Mechanical Finite-Element Model with Application to Initial Solidification." Ph.D. Thesis, University of Illinois at Urbana-Champaign, (1996).

- Austenite (Kozlowski model III):

$$\dot{\varepsilon}\left(\mathrm{s}^{-1}\right)=f(C)\left[\sigma-f_1(T)\varepsilon\left|\varepsilon\right|^{f_2(T)-1}\right]^{f_3(T)}\exp\left(-\frac{4.465\times10^4(K)}{T}\right)$$

$$f_1(T)=130.5-5.128\times10^{-3}T$$

$$f_2(T)=-0.6289+1.114\times10^{-3}T$$

$$f_3(T)=8.132-1.54\times10^{-3}T$$

$$f(C)=4.655\times10^4+7.14\times10^4C+1.2\times10^5C^2$$

- δ-ferrite (Zhu modified power law):

$$\dot{\varepsilon}\left(s^{-1}\right)=0.1\left|\sigma/f(C)(T/300)^{-5.52}(1+1000\varepsilon)^m\right|^n$$

$$f(C)=1.3678\times10^4(C)^{-5.56\times10^{-2}}$$

$$m=-9.4156\times10^{-5}T+0.3495$$

$$n=1/1.617\times10^{-4}T-0.06166$$

- Liquid and mushy zone:
  - Treat as low yield stress, low elastic modulus, perfectly-plastic solid

T in Kelvin, σ in MPa, C in weight % C

Evaluation of Kozlowski Model

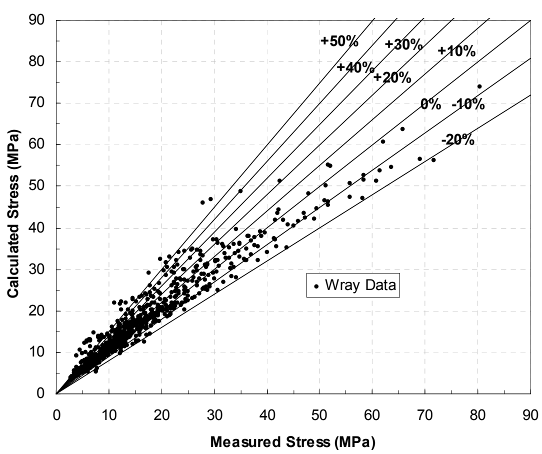

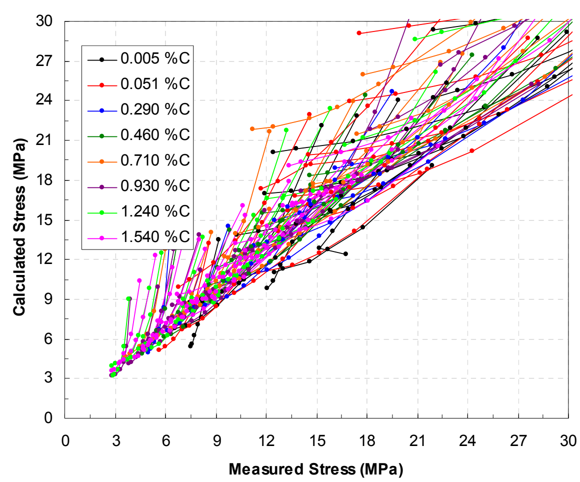

±10%: 46% of data

±20%: 75% of data

Kozlowski Model is generally accurate, except for:

- **Low stress, high strain**
- **High stress, low strain**

Traveling Slice Analysis

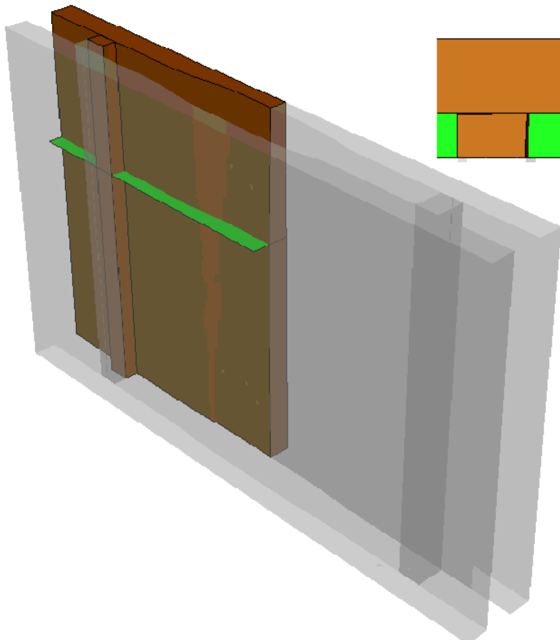

Casting Speed = 4.5 m/min

Oscillation Stroke = 6.4 mm

Oscillation Freq. = 305 cycles/min

Shown at Half Speed

Finite Element Mesh

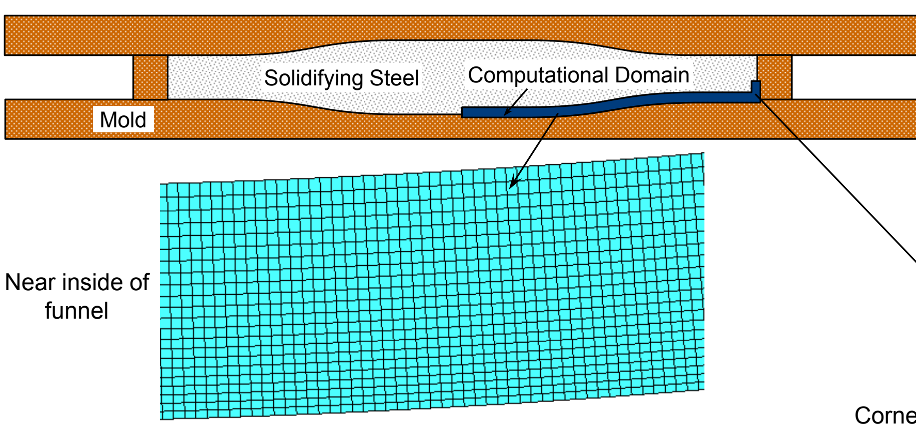

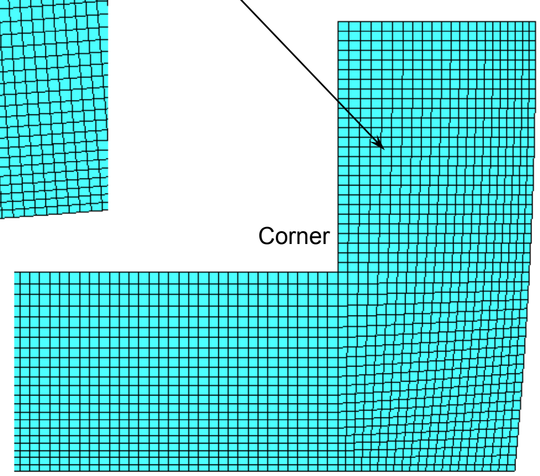

- Standard 4-node heat transfer elements
- Hybrid formulation of generalized plane strain mechanical elements
- Fixed mesh, about 60000 nodes

Process Parameters

Casting speed	5.5 m/min	217 ipm
Carbon content	0.045 %wt	
Pour temperature	1545.0 ºC	2813 ºF
Strand width	1200 mm	47”
Narrow face taper	1.0 %/m	
Meniscus depth	104.2 mm	4”
Time in mold	10.86 s	

Heat Flux Profiles:

Interfacial Thermal Boundary Condition

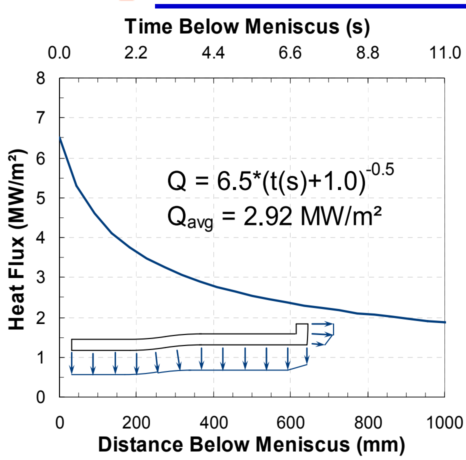

- Heat flux uniformly applied around most of the perimeter
- Decrease heat flux at corner to account for gap formation (linear drop to 50% over 20 mm)
- Average Q matches measurements

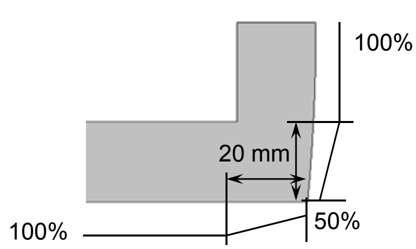

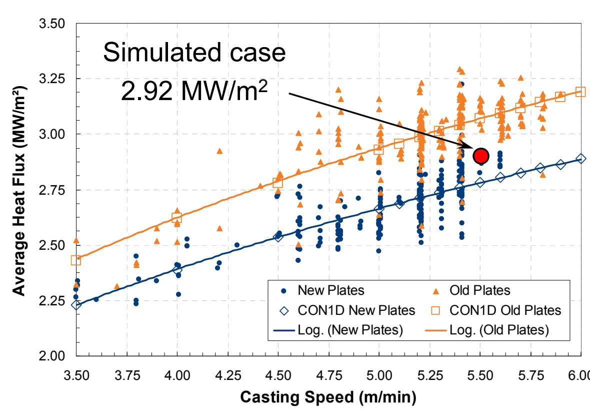

[Santillana *et al.*, AISTech 2007]

Ferrostatic Pressure and Mold Wall Movement: Mechanical Boundary Conditions

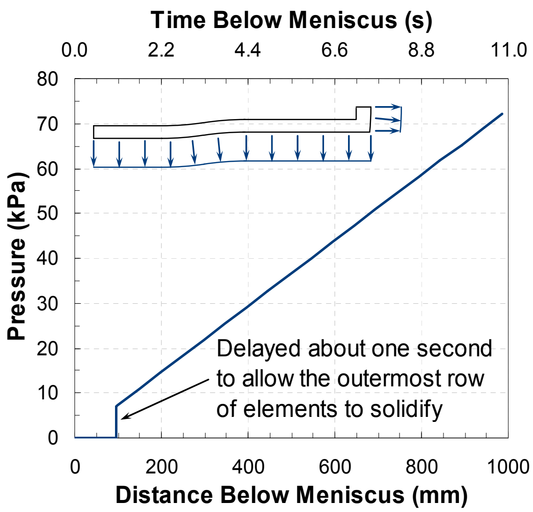

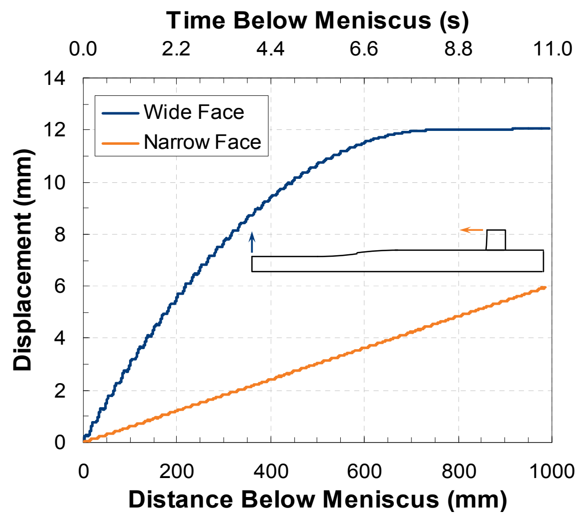

Ferrostatic Pressure **Hot Face Displacement**

Model Verification:
Properties, Parameters, and Boundary Conditions

- J.H. Weiner and B.A. Boley, "Elasto-Plastic Thermal Stresses in a Solidifying Body." *Journal of the Mechanics and Physics of Solids*, **11** (1963), No. 3. pg 145-154.

Property/Condition	Value	
Density	7500.0	kg/m^3
Specific heat	661.0	J/(kg·ºC)
Latent heat	272.0	kJ/kg
Thermal conductivity	33.0	W/(m·ºC)
Thermal expansion coefficient	20.0E-6	m/(m·ºC)
Poisson's ratio	0.3	--
Initial temperature	1495.0	ºC
Liquidus temperature	1494.48	ºC
Solidus temperature	1494.38	ºC
Mold temperature	1000.0	ºC
Yield stress at mold temp.	20.0	MPa
Yield stress in liquid material	35.0	kPa
Elastic modulus in solid	40.0	GPa
Elastic modulus in liquid	14.0	GPa

Thermal Boundary Conditions

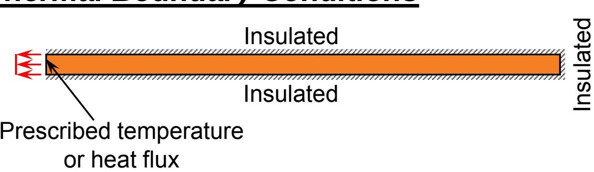

Mechanical Boundary Conditions

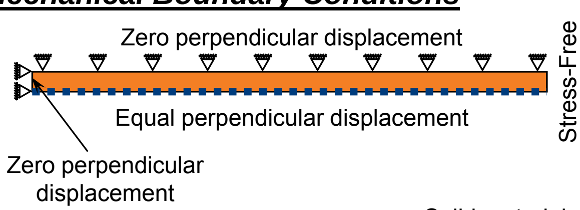

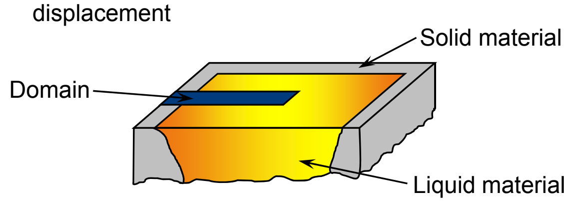

Model Verification: Temperature Solution

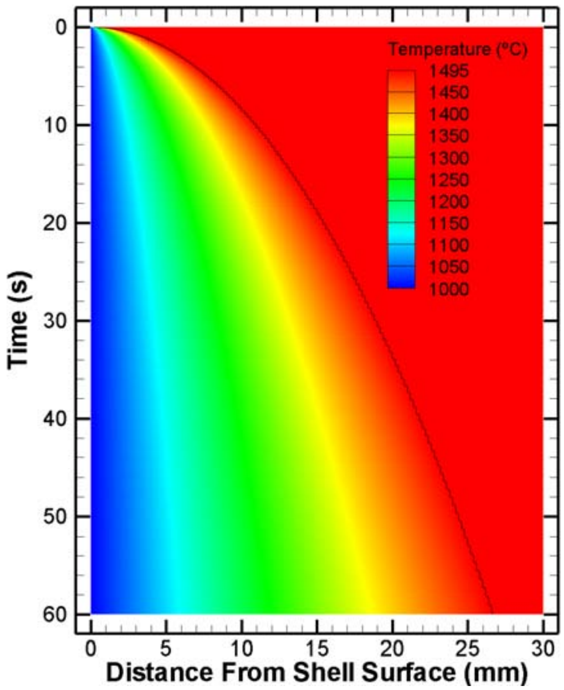

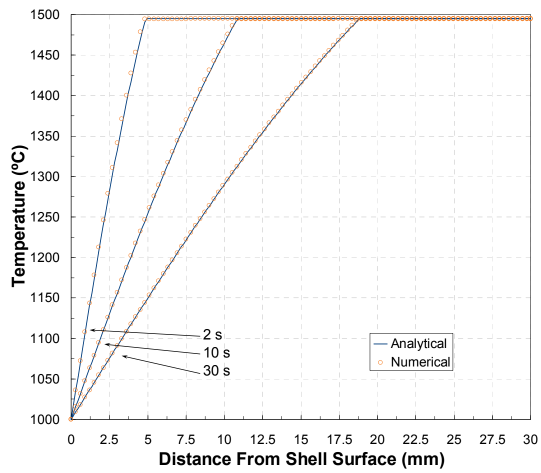

Model Verification: Stress Solution

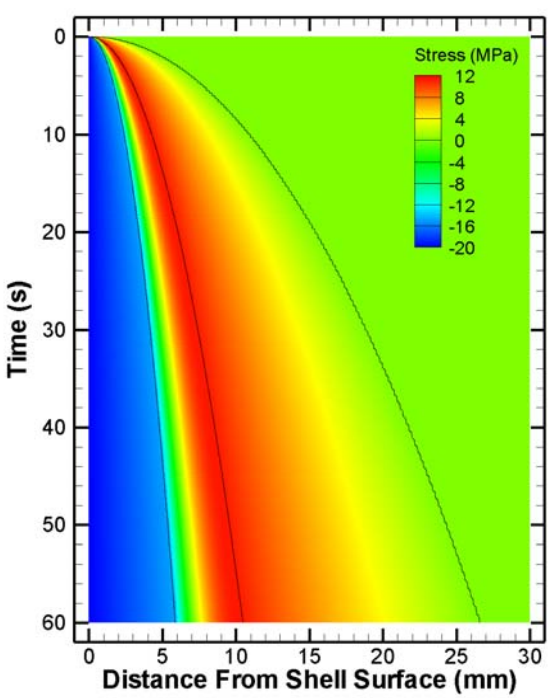

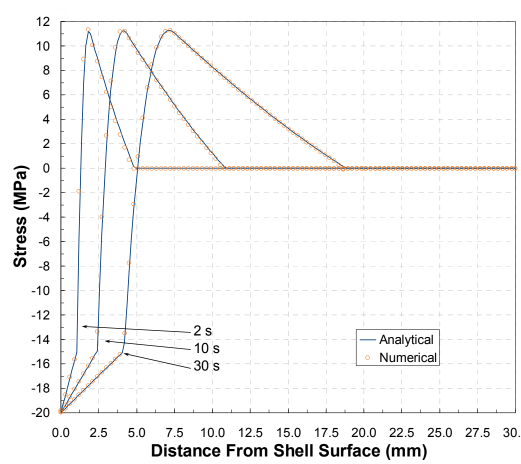

Temperature Results

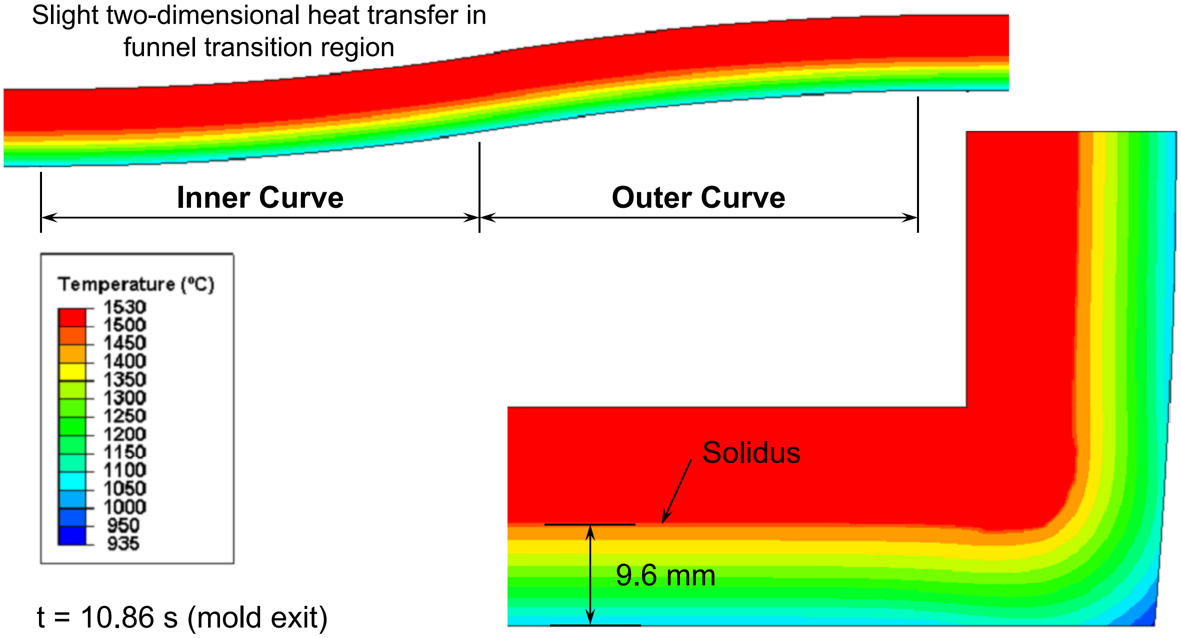

t = 10.86 s (mold exit)

Temperature Solution

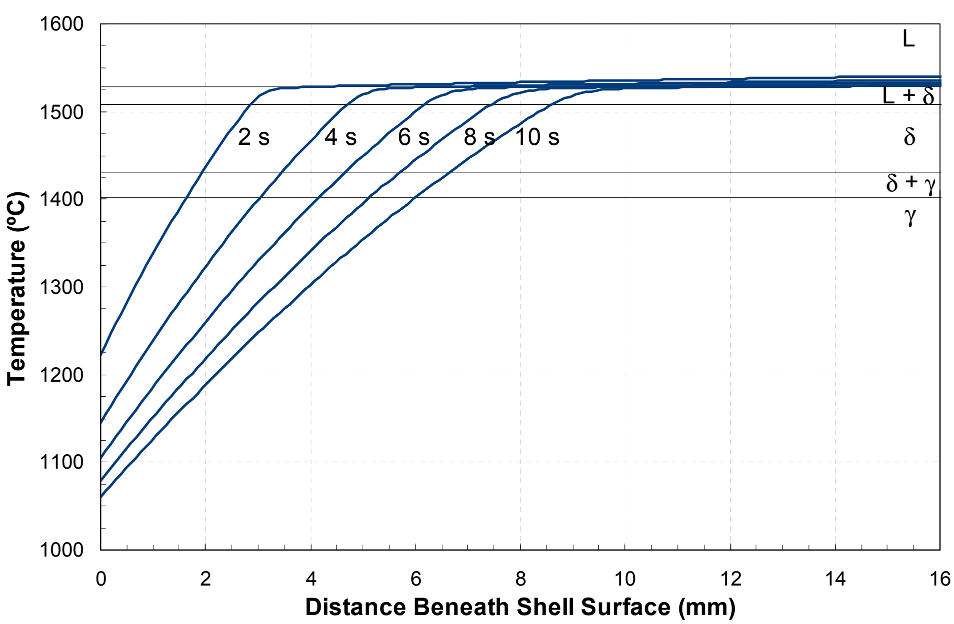

Stress Profiles and Histories
Through Thickness in Flat Regions

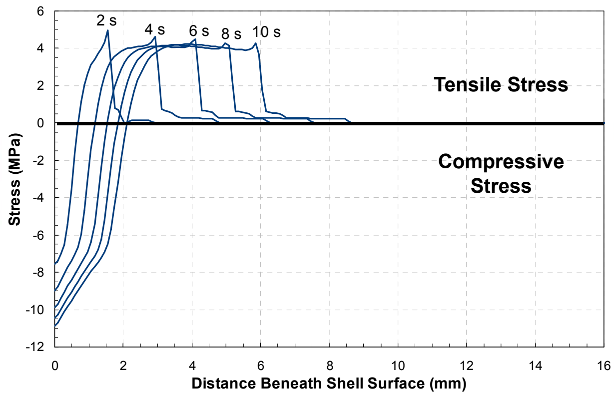

- After initial tensile load, surface stays in compression
- Solidification front is always under tensile loading
- Net stress through-thickness is always zero

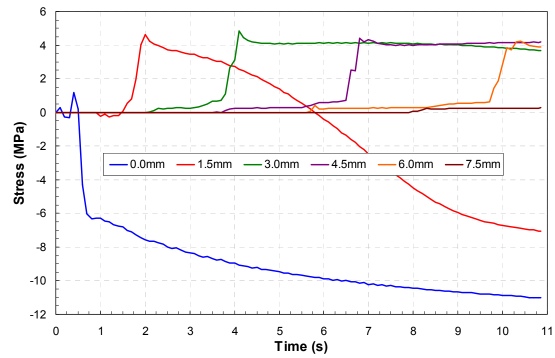

- Soft delta-ferrite unable to carry a substantial load
- Stress peaks after transition to the austenite phase
- By mold exit, only the first 2 mm of the shell are in compression

1.5 mm = 0.06”

Surface Stress Around Perimeter: Effect of Funnel Width

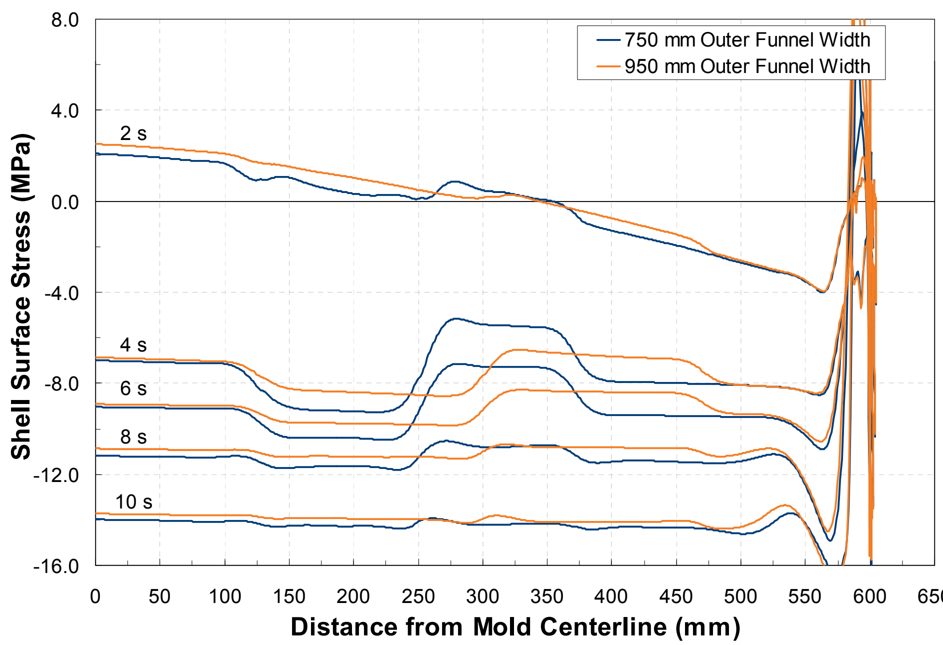

Stress *Near* Solidification Front: Effect of Funnel Width

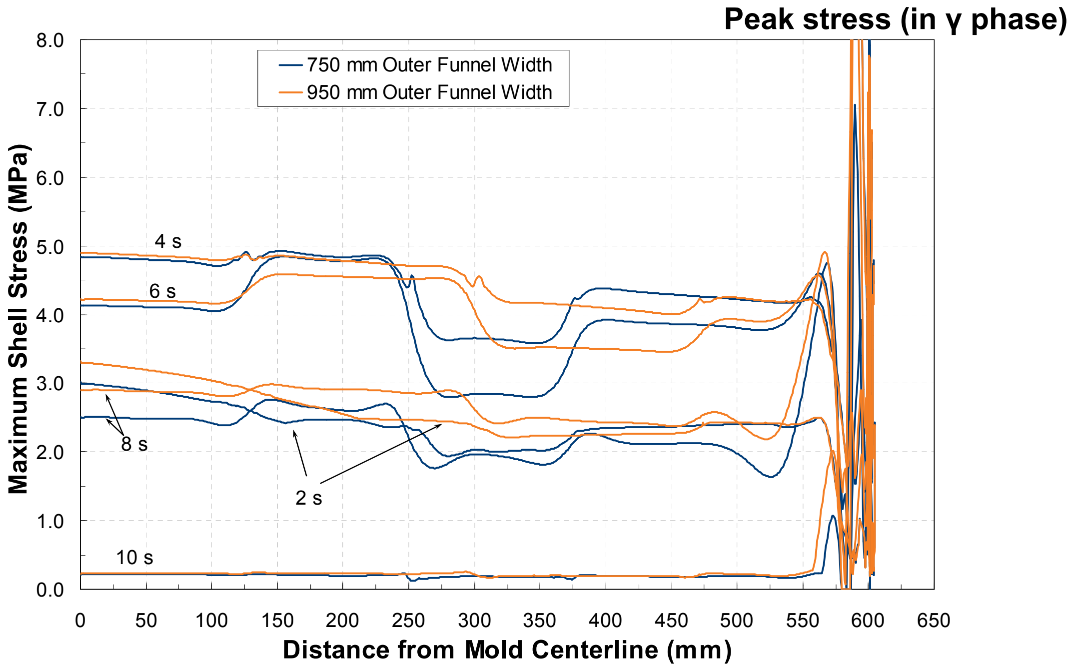

Funnel Bending Effect

- A unique attribute of funnel molds is that the steel shell is ***significantly*** bent as it slides down the mold

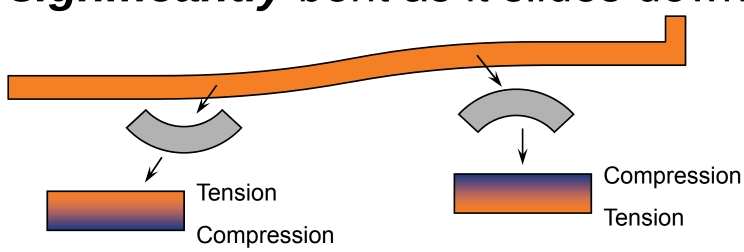

- Beam theory from solid mechanics can elucidate the important parameters in the phenomenon

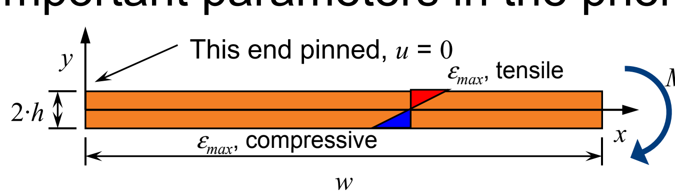

$$\varepsilon_x = -\frac{y}{R}$$

[R.C. Hibbeler, *Mechanics of Materials*, 5e, 2003]

Analytical Bending Model: Comparison with Numerical Model

- Take the difference between bending a beam to the funnel radius at the meniscus and the funnel radius at some other depth:

$$\varepsilon_{bending}(z)=\frac{\delta(z)}{r(z_{meniscus})}-\frac{\delta(z)}{r(z)}=\delta(z)\left(\frac{r(z)-r(z_{meniscus})}{r(z)\,r(z_{meniscus})}\right)$$

$$r(z)=\frac{crown(z)}{4}+\frac{(outer\ \ funnel\ width-inner\ \ funnel\ width)^2}{16\cdot crown(z)}$$

δ = distance from neutral axis ≈ shell thickness

- Compare with results of 2D model with the thermal effects subtracted

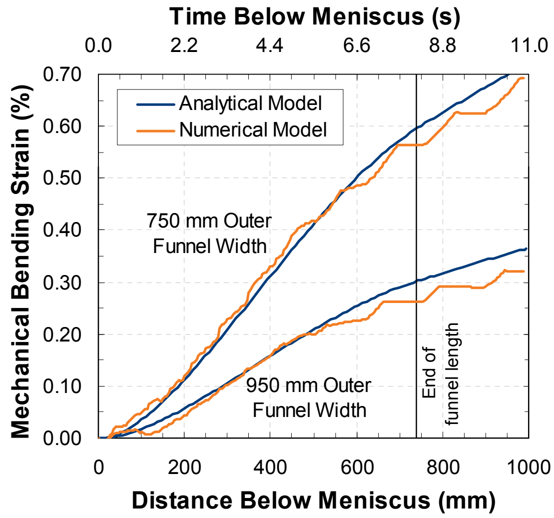

Bending Strain on Solidification Front

Analytical Bending Model

Larger total funnel width = Larger radius = Lower bending strain and strain rate

Shallower funnel = Larger radius = Lower bending strain and strain rate

Longer Funnel = Increases strain near bottom of funnel (larger radius for more time), but lowers strain rate

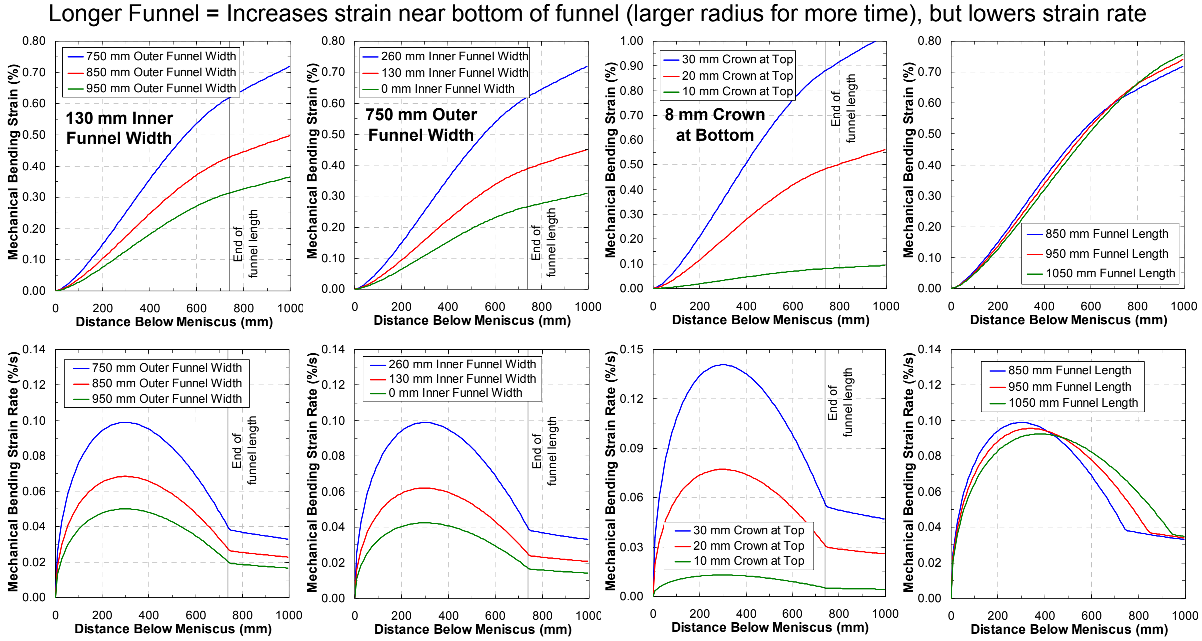

Subsurface Hot Tears

- Typical solidification stresses put tension on the solidification front
  - Tension increased by bending effect in inner curve region, thus higher risk of hot tearing
- Critical hot tearing strain quantified by Won:

$$\varepsilon_c = \frac{0.02821}{\dot{\varepsilon}^{0.3131} \cdot \Delta T_B^{0.8638}}$$

Won *et al.*, *Metall. Mat. Trans.*, **31B**:4 (2000), pg. 779

- Brittle temperature zone (BTZ):

$$\Delta T_B = T(f_s = 99\%) - T(f_s = 90\%)$$

- Average inelastic strain rate in BTZ:

$$\dot{\varepsilon} = \frac{\varepsilon(f_s = 99\%) - \varepsilon(f_s = 90\%)}{t(f_s = 99\%) - t(f_s = 90\%)}$$

Subsurface Hot Tears

- Extremely fine mesh required to apply Won model (0.06 mm element size is insufficient)
  - Use 1D numerical model to calculate temperatures and inelastic strain profile history in flat regions of mold
  - Add bending effect with analytical model
- Low-carbon steels exhibit strong numerical noise
  - Use a higher carbon grade (0.07%C) to reduce effect
  - High-carbon grades are also more crack-sensitive
- Define “damage index” as ratio of actual damage strain to critical damage strain (crack forms at unity)

$$\varepsilon_{dmg} = \varepsilon(f_s = 99\%) - \varepsilon(f_s = 90\%) \qquad D = \varepsilon_{dmg} / \varepsilon_c$$

Subsurface Hot Tears

- No hot tears will form under normal operation
  - Bending effect increases likelihood of cracks
- Most likely place is just a few mm subsurface
- Funnels more susceptible to hot tears:
  - Narrower funnel width (higher bending strain)
  - Deeper crowns (higher bending strain)
  - Longer (higher strain rate when mushy zone is large)

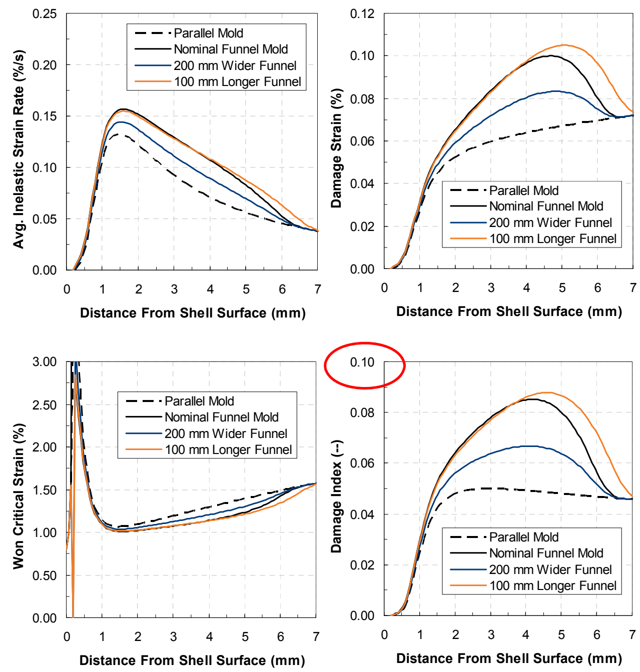

Pushing the Shell

- As the crown decreases, the steel shell is pushed inward to the SEN and outward to the narrow faces
  - Opposed by friction and excessive narrow-face taper
  - Affected by solidification shrinkage (possibly compensating)
  - Most noticeable at early times before opposing effects are strong, but always present

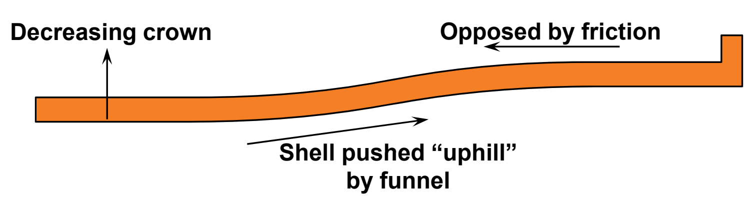

Interfacial Gaps

- Predicted gaps are mechanical effects, due to no coupling of mechanical model to heat transfer model (coupled model would have larger gaps)
- Small gaps in the inner curve region
  - "Shell pushing" encourages good contact
- Larger gaps in the outer curve region
  - Shrinkage from outer flat region is resisted by "shell pushing"
- Both influenced by bending effect
- Shrinkage minus "pushing" meets somewhere in the middle of the funnel

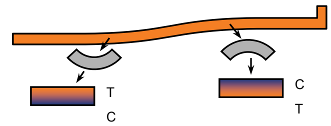

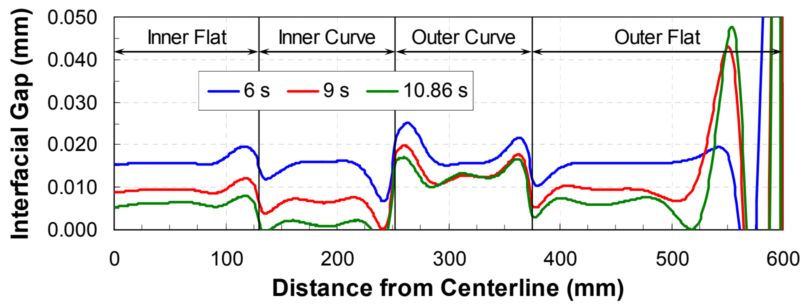

Depression Mechanisms

- Inside curve:
  - Friction + bending pins the shell at the transition points
  - Mold may induce buckling if local shell shrinkage is not enough to match the mold perimeter length change

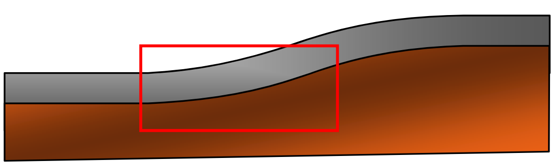

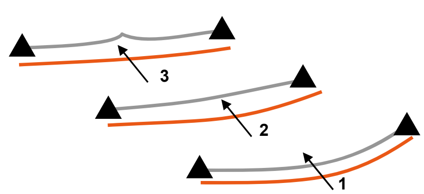

- Outside Curve
  - Friction + bending pins the shell at the inside/outside curve transition point
  - Excessive NF taper causes the shell to lift off the mold surface, reducing heat transfer
  - Bending (funnel and ferrostatic pressure) causes tensile stress on surface, leads to necking

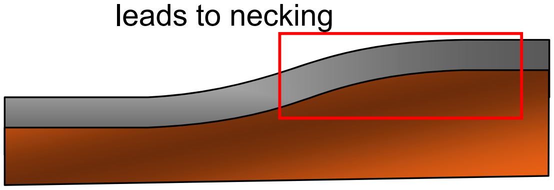

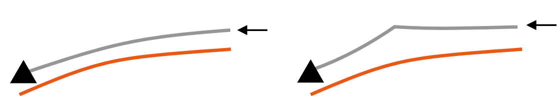

Tangential Displacement

- Project the *incremental* displacement vector onto a vector tangent to the mold surface
  - Neglects the “global” mold displacement, but includes the effects of the shell sliding around the funnel “corners”

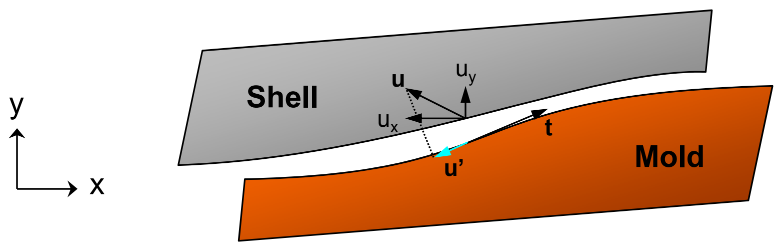

Surface Displacement: Effect of Funnel Width

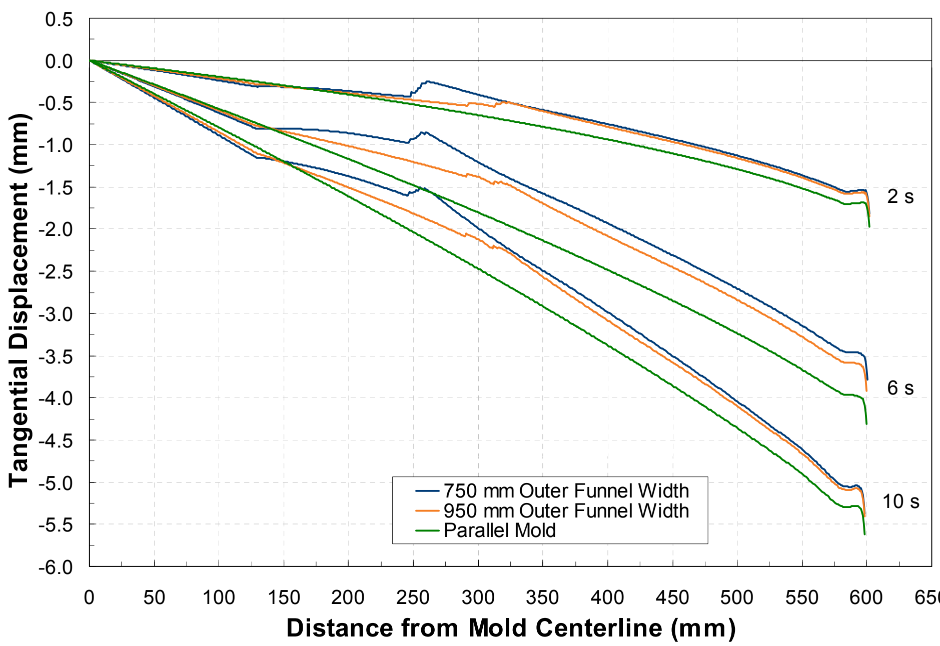

Surface Trajectories

Parallel Mold, no Friction

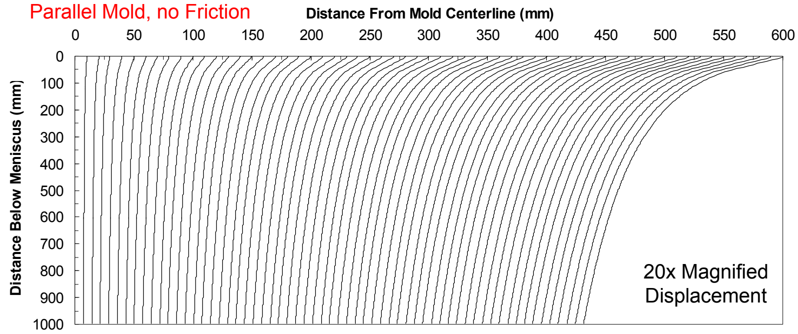

Parallel Mold, with Friction

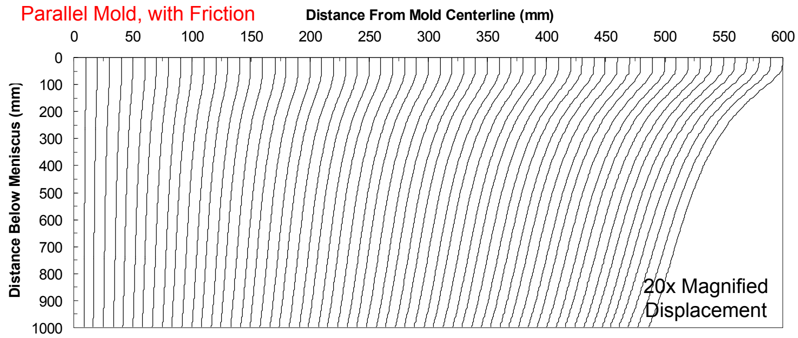

- Put markers at the meniscus that draw a line on the mold as they move with the shell
- Friction plays a very important role on shell shrinkage (1D heat transfer model is insufficient to predict mold tapers)
- Friction holds the shell in place at early times by overpowering shrinkage

Surface Trajectories

Parallel Mold, with Friction

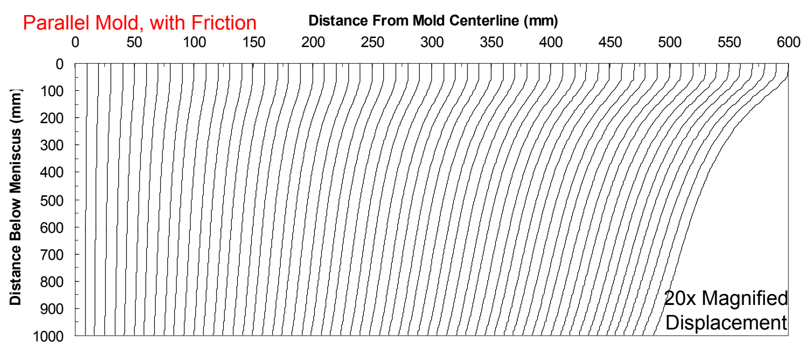

Funnel Mold, with Friction

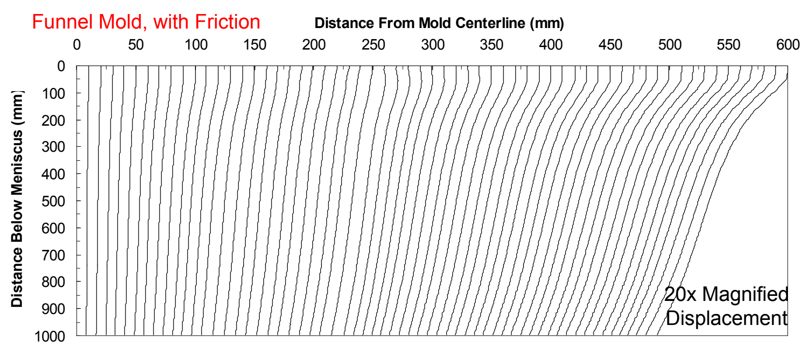

- Inside curve trajectories are spaced further apart (not shrinking as much as it wants too)
- Outside curve trajectories are spaced closer together (shrinking more than it wants to)
- Outside curve shows initial movement towards the narrow face
- Large gap at inside/outside transition suggests outside curve bending + friction pulls the shell towards the narrow faces

Conclusions

- A larger funnel radius provides:
  - More uniform heat transfer
  - Smaller bending effect in the transition region
  - Lower tendency to form subsurface hot tears
- A "*better*" funnel (with respect to depression-type LFCs) has a wide funnel and small crown

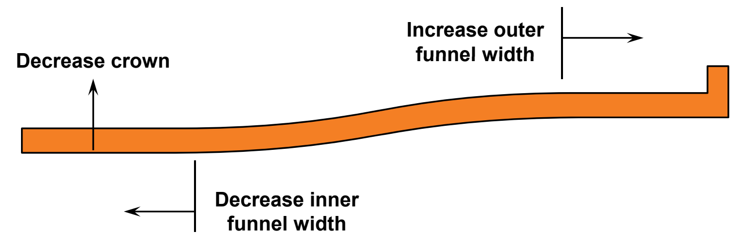

- Depression-related LFCs are also affected by friction, and narrow-face taper
- Many other phenomena can cause LFCs

Acknowledgements

- Continuous Casting Consortium Members (ABB, Arcelor-Mittal, Baosteel, Corus, Delavan/Goodrich, LWB Refractories, Nucor, Nippon Steel, Postech, Steel Dynamics, ANSYS-Fluent)
- Dr. Seid Koric, Dr. Chunsheng Li, Dr. Hong Zhu
- Begoña Santillana, Gert Abbel, Arnoud Kamperman, Jean Campaniello, Frank Grimberg
- National Center for Supercomputing Applications (NCSA) at UIUC – "Tungsten" and "Abe" clusters
- Dassault Simulia, Inc. (ABAQUS parent company)